GEOMETRIC CHARACTERISTICS, COMPOSITION AND STRUCTURE OF COATINGS OF WC-TIB2-B4C- NI-CR-B-SI-C ELECTRODES FORMED ON 3D PRINTING TITANIUM AND STEELS BY CONTACTLESS ELECTROSPARK DEPOSITION

G. Kostadinov[1], T. Penyashki[1], A. Nikolov[2], R. Dimitrova[2], V. Kamburov[2], M. I. Petrzhik[3], B. Elenov[1], I. Mortev[1], E. Dimitrova[1]

[1]ISSAPP "N.Pushkarov", Agricultural Academy – Sofia, Bulgaria

[2]Technical University of Sofia, Bulgaria

[3]NUST MISIS, Moscow, Russia

Abstract

The object of the present work are the surface properties of technical titanium produced by 3D printing - Direct Metal Laser Sintering (DMLS) with subsequent treatment by local electrospark deposition with a rotating electrode (LESD). The layering was performed with electrodes of multicomponent hard alloys based on WC with additives from B_4C, TiB_2 and Ni-Cr-B-Si-C and of AlSi alloys. The influence of the LESD process parameters on the roughness, thickness, composition and structure of the coatings was studied by profilometric, metallographic, XRD, SEM and EDS methods. High-density coatings with different roughness and thickness have been obtained, which can be changed by changing the LESD modes in the range Ra=1.25÷3.5μm, δ=6÷20μm and microhardness 9÷14.0 GPa. Friction tests have shown that the wear of coated surfaces is up to 4 times lower than uncoated. On the basis of the experimental data, appropriate process parameters and electrodes have been determined, allowing to obtain coatings with purposeful synthesized of new phases and crystal-amorphous structures, and with predetermined thickness and roughness and higher hardness, and wear resistance than those of substrates.

Keywords: *3D printing, Direct metal laser sintering DMLS, Local electrospark deposition - LESD, titanium alloys, roughness, microhardness, wear, wear resistance*

1. INTRODUCTION

Currently, the improvement of the surface properties of metal products obtained by the most widespread in practice additive technologies for 3D printing of metals - selective laser sintering (SLS) and Direct Metal Laser Sintering - DMLS) (Aloshin et al 2016 , Bogers, Hadar & Bilberg 2016, Laplume, Petersen & Pearce 2016, Freedman 2019; Monkova et al. 2019) can be done in one of the following main ways:

- By selecting appropriate modes for construction (laser power, energy distribution in the laser spot, laser beam scanning speed and trajectory, distance between scanning tracks, powder material layer thickness, platform preheating, shielding gas type (Zaytsev & Polupan 2020; Shipley,McDonnell & Culleton 2018, Sufiyarov et al 2018). But the impossibility of good cleaning, satisfactory reduction of roughness, and shaping of surfaces are still a serious obstacle to the application of this technology for the manufacture of all-metal structures.

- By laser re-melting. According the method, proposed by (Yasa & Kruth 2011), each layer is "processed", the laser twice. As a result, the porosity is reduced, but the time to build the part is doubled.

- By additional treatments - mechanical (grinding, manual polishing, shot blasting, cutting and pressing), electrochemical, electroerosion etc. However, these treatments require appropriate machines, technologies, equipment and tools, as well as the use of specific technological regimes for different materials and shapes of products and leaving allowances for the further processing, which is associated with excessive increases in time and costs. Moreover, the machining of parts of titanium alloys, high-alloy chromium-nickel steels and intermetallic compounds is a labor-intensive operation due to their poor machinability.(Bogers, Hadar & Bilberg 2016, Laplume, Petersen & Pearce 2016, Freedman 2019)

- By adding a new layer on top of the 3D surfaces. According to most researchers (Sufiyarov et al 2018, Laplume, Petersen & Pearce 2016, Freedman 2019, Ramos-Grez & Bourell 2004, Tsvetkova et al 2020, Grabarczyk 2020) one of the most promising guidelines for improving the quality of 3D surfaces and increasing their wear resistance is the creation of surface layers with higher physical-mechanical and tribotechnical properties, and electrochemical, galvanic, thermochemical, electrophysical and other methods are approved as suitable.

Among these methods, the lightest, cheapest, most accessible, universal and highly ecological is electrospark deposition ESD (Penyashki et al 2020, Penyashki & Kostadinov 2013, Mukanov, Kudryashov & Petrzhik 2021, Kostadinov et al. 2021, Penyashki et al. 2022). The method has a number of advantages (Penyashki et al. 2020, Mukanov, Kudryashov & Petrzhik 2021,Kostadinov et al. 2021, Penyashki et al. 2022), the main of which are: its simplicity, low cost of equipment, easy technology, high adhesion with the base, insignificant heating and lack of thermal deformation of the layered products, low energy consumption and ease of execution of technological operations, the possibility of local processing of any surface, even of the most complex shape. The ESD coating changes the deposited surface both in terms of geometry and topography, as well as in terms of its composition, structure and properties.

The efficiency of ESD is a function of the electrode materials and equipment used. Therefore, the

question arises of using new electrode materials, as well as of establishing the influence of the process parameters on the characteristics of the coatings applied with the new materials and on the performance characteristics of the binder material, which will allow to determine effective ways to control the performance properties of layered surfaces.

In this regard, the aim of the present work is to investigate the influence of ESD parameters with low energy pulses and the electrodes used on the roughness, morphology and wear resistance of the coatings with a view to improving the quality of the DLMS surface layer.

2. MATERIALS AND METHODS

2.1. Materials, Equipment for ESD and Deposition Conditions

- *Substrate.* Model plates with different roughness of titanium alloy Ti6Al4V (Gr5) and of technical titanium Ti-GR2 (Aisi UNS R R56200 and R50400) are used for substrate. Carbon steel 1.2709 produsedby DMLS with composition Fe- base, Ni - 18-19 %, Mo 4,7-5,2%, Co 8,5-9,5 %, C 0,03%, with sizes 10×10×4 were also used for comparison.

- *Equipment for ESD.* High-frequency and low-energy mechanized variant of ESD is used - local contactless electrospark deposition (LESD) (Antonov, Panayotov & Lyutakov 1980) with low pulse energy, with electronic system for tracking and maintaining the interelectrode distance, and with a controlled speed of movement along the X and Y axes at layering of the treated parts . This equipment ensures the production of coatings with higher density and uniformity, with lower roughness and with significantly improved repeatability of quality characteristics.

LESD deposition is performed at 3 modes – at single pulse energy E and parameters given in Table 1. The application of the coatings is carried out with cylindrical rotating electrode with a diameter 1.8 mm. The performance of the deposition is 0.5÷0.6 mm/s, Electrode rotation speed is 1200 rpm, Circuit voltage U= 90V.

Table 1. Mode Parameters at LESD – Device "Elfa 541"

N	Pulse current amplitude - I, A	Pulse duration – Ti, μs;	Capacitance – C, μF;	Pulse frequen-cy-f, kHz	Passages of the electrode	Single pulse energy, J
1	12,8	8	0.68	12.5	3	0.01
2	16	12	1	8	3	0.02
3	24.4	20	4.4	5	3	0.04

2.2. Electrode materials

Composite multicomponent hard alloys with designations and composition given in Tables 2 and 3 were selected to provide both high wear resistance, such higher amount of transfer from the liquid phase and obtaining new additional wear-resistant compounds and phases in the process of forming the coatings (Penyashki, Radev et al 2020, Penyashki, Radev et al 2019, and Kamburov et al 2021). The selected multi-metallic materials differ from the known ones in that, in addition to WC, they additionally contain highly wear- and corrosion-resistant TiB_2 and B_4C, and the solder mass is made of the multi-component Ni-Cr-Co-B-Si-C system, which ensures a higher transfer, higher coating density, strong bond with the base, high abrasion and corrosion resistance.

Type of ESD electrode	Chemical composition
NWW10T10B10	50%WC+10%TiB_2+10% B_4C+(Ni-Cr-B-Si-C)-bal.
NWW15T20B10	55%WC+20%TiB_2+10% B_4C+(Ni-Cr-B-Si-C)-bal.
NWW15T20	40%WC+20%TiB_2+15% B_4C+(Co-Cr-Ni-B-Si-C)
AlSi9	9%Si +Al

Table 2. Composition of used ESD electrodes

Element	C	Si	Cr	Fe	B	Ni
Composi-tion,%	0.5	3	12	4	3.5	balance

Table 3. Chemical composition of the bonding powder mixtures Ni-Cr-B-Si-C

Layering electrodes of low-melting AlSi9 alloys (Mukanov, Kudryashov & Petrzhik 2021, Penyashki et al. 2022), recommended by (Mukanov, Kudryashov & Petrzhik 2021, Penyashki et al. 2022, MILLIGAN, HEAD, & BROCHU 2010, Cadney et al. 2009), which provide the forming of a liquid melt, protection against oxidation due to the presence of silicon, as well as targeted synthesis of new reinforced phases and production of nanostructured coatings with amorphous phases with high wear resistance and performance properties were used as reference for comparison with the resulting coatings from the electrodes of "NWW" type.

2.3. Types of research, Methodology of measurements, Research Equipment

- The parameters of roughness Ra, Rz, Rq and Rt and thickness of the resulting coatings are measured by using profilometers AR-132B at EN ISO 13565-2:1996) standart.

- The morphology and topography of the LESD layers were examined with a scanning electronic microscope SEM "EVO MA10 Carl Zeiss".

- The measured microhardnesses were performed with a Zwick 4350, Germany hardness tester, according to ISO 6506-1: 2014, at a load of 2 N with a Vickers indenter diamond prism and a penetration depth of 2-3 μm.

- The phase identification, the distribution of elements in the surface layer, and microstructural analysis of the coatings were performed with a X-ray diffractometer Bruker D8 Advance in “Cu Kά” radiation.

- The X-ray energy dispersion microanalysis was performed with a built-in X-ray energy dispersion microanalyzer EDX system "Bruker" to a scanning electron microscope SEM "EVO MA10 Carl Zeiss".

- The tribological properties and wear resistance of the coatings are investigated by comparative tests of friction with tribotester type "Thumb-on disk" under dry surface friction with hard-fixed abrasive particles and at loads P 5 and 10 N. The wear characteristics test method consists in measuring the mass wear “m” of the samples for a specific friction path “L” (friction cycles) under constant conditions - load “P” and glide speed “V”.

The following wear characteristics were calculated:

- Mass wear - $m = m_O - m_i$, mg

- Wear intensity - the amount of wear per unit of friction work: $W = \frac{m}{PL}$, where m is the wear of the solid for the test time, P - the normal load, L - the friction path passed.

- Wear resistance (W_r): Reciprocal value of the wear intensity.

3. RESULTS AND DISCUSSION

3.1. Coating characterization – Roughness, thickness, structure and micro-hardness

The average values of surface roughness parameters Ra, Rz, Rq, Rt, the thickness δ, and microhardness HV of coatings, obtained are shown in Table 4 and 5.

Table 4. Roughness Ra,Rz,Rq,Rt, thickness δ and microhardness HV of coatings on DMLS Ti6Al4V substrates

№	Coating electrode	Ra, μm	Rz, μm	Rq, μm	Rt, μm	δ, μm	HV, GPa
0	substrate Ti6Al4V	7.54	21.23	7.8	21.47	-	3.75
1	NWW10T10B10, E=0.02 J	3.47	9.8	3.29	10.48	10.75	9.85
2	NWW10T10B10, E=0.04 J	4.81	13.59	4.91	14.22	18.53	12.34
3	NWW15T20B10, E=0.02 J	3.56	10.43	3.88	10.84	9.87	12.83
4	NWW15T20B10, E=0.04 J	4.25	11.95	4.35	12.05	14.85	12.45
5	NWW15T20, E=0.02 J	3.43	9.62	3.47	9.72	9.54	11.87
6	NWW15T20, E=0.04 J	4.64	13.12	4.49	16.63	14.66	12.22
7	ASi9, E=0.02, 2 pass	2.29	6.47	2.3	6.54	6.7	8.03

7	ASi9, E=0.03, 2 pass	2.46	6.9	2.48	6.97	8.6	7.86
8	ASi9, E=0.04, 2 pass	3.28	11.17	4.02	11.38	9.55	9.43
9	AK9, E=0,04 , 3 pass	3.37	11.77	4.37	12.1	11.11	9.67

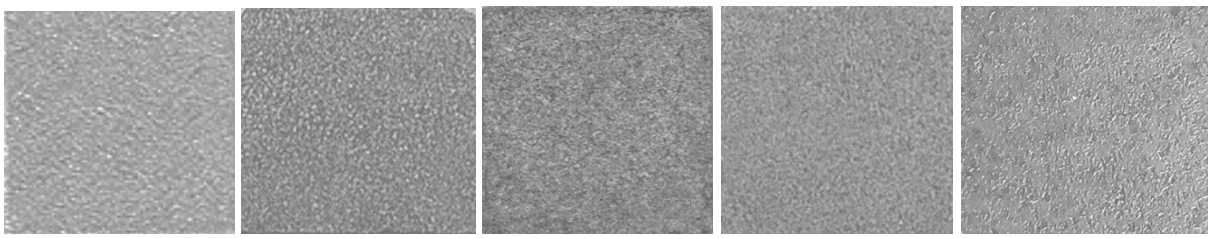
The coatings from NWW electrodes are obtained with 3 passes of electrodes

Table 5. Roughness Ra, Rz, Rq, Rt, thickness δ and microhardness HVof coatings on DMLS 1.2709 steel substrates

№	**Coating electrode**	**Ra, µm**	**Rz, µm**	**Rq, µm**	**Rt, µm**	**δ, µm**	**HV, GPa**
1	substrate 1.2709	10.28	29.04	9.59	31.19	-	4.47
2	AlSi9, E=0.02 J	3.12	8.82	3.24	8.91	9.15	8.84
3	AlSi9, E=0.04 J	4.15	11.75	4.35	11.85	12.53	9.66
4	NWW10T10B10, E=0.02 J	3.62	10.2	3.32	10.33	15.87	12.55
5	NWW10T10B10, E=0.04 J	4.64	13.12	4.49	16.63	21.25	12.59
6	NWW15T20B10, E=0.02 J	3.56	10.43	3.89	12.24	11.47	13.82
7	NWW15T20B10, E=0.04 J	5.02	14.2	5.475	15.35	16.63	13.89
8	NWW15T20, E=0.02 J	3.42	9.67	3.82	9.77	10.82	12.83
9	NWW15T20, E=0.04 J	4.81	13.6	4.52	14.32	15.65	12.86

The characteristic appearance and topography of the surface of the coatings is shown in Figs. 1, 2 and 3. They are compared with those of coatings from ASi9 electrodes.

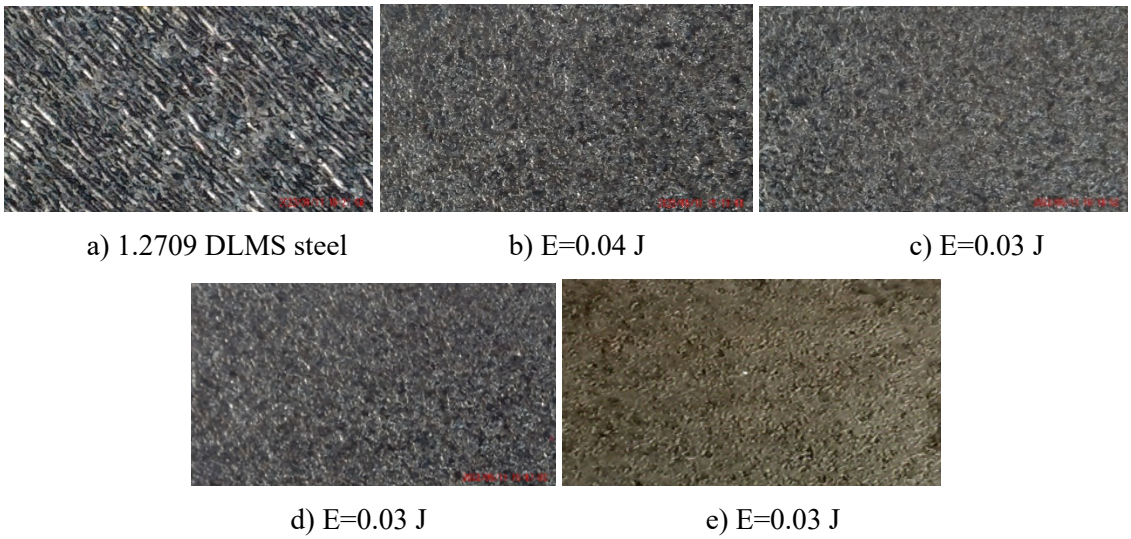
Fig. 3 displays the change of the roughness parameters of the coatings Ra, Rz, Rt depending on the energy of the single pulses. Dense and uniform coatings, similar in structure formed mainly by the liquid phase were obtained with both „NWW“ and AlSi electrodes. The coating parameters can be changed by changing the pulse energy in the range of thickness δ=5-20 µm and microhardness HV=7 to 14 GPa. The resulting surfaces have a specific relief different from the original. It can be seen that their roughness is lower than that of the substrate. The standard deviation from the mean value after ESD and LESD also has significantly lower values than those of the initial samples.



a) Ti6Al4V b) E=0.04 J c) E=0.04 J d) E=0.02 J e) E=0.02 J

Fig. 1. View of model plates from Ti6Al4V before and after LESD:

a) DLMS substrate, Ra initial ≈8µm; b) LESD with NWW10T10B10 electrode, coating Ra≈4.8 µm; c) with NWW15T20B10 - Ra≈4,5 µm; d) with NWW10T10B10 -Ra≈3 µm; e) with AlSi9 -Ra≈2,5 µm



a) 1.2709 DLMS steel b) E=0.04 J c) E=0.03 J

d) E=0.03 J e) E=0.03 J

Fig. 2. Top view of model plates from 1.2709 steel before and after LESD: a) DLMS substrate, Ra initial ≈10μm; b) LESD with NWW10T10B10 electrode, coating Ra=4.6 μm; c) LESD with NWW15T20B10 electrode Ra≈3,6 μm; d) LESD with NWW15T20B10 electrode Ra≈3,9 μm; e) LESD with AlSi9 electrode Ra ≈3μm.

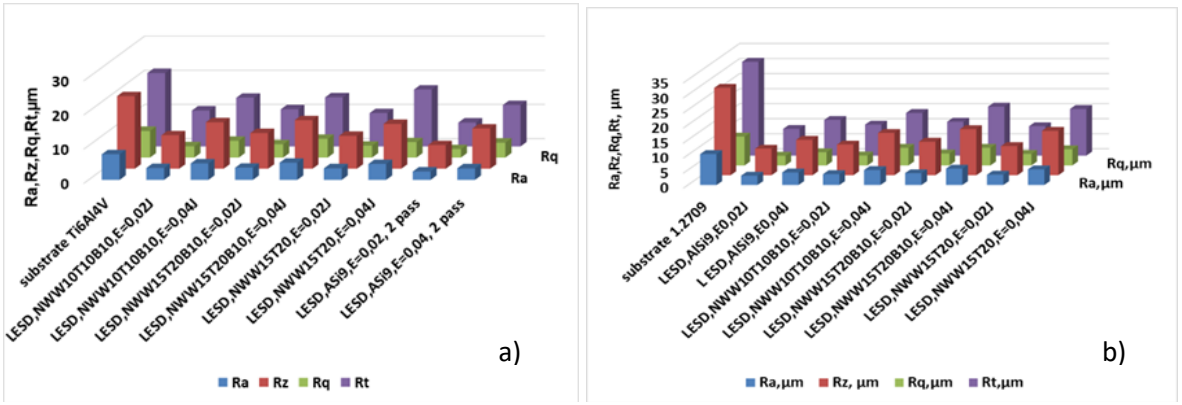


Fig. 3. Roughness parameters Ra, Rz,Rq,Rt of LESD coatings on DLMS Ti6Al4V alloy: a), and 1.2709 steel; b) vs two modes of the pulse energy

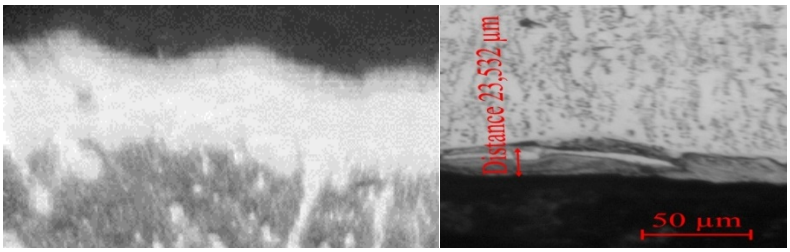
The comparison of the measured roughness - Tables 4 and 5, showed that after LESD the parameter Ra decreases to values Ra=2.5 to 5 μm. The other studied roughness parameters also significantly decrease. In the low pulse energy modes (0.02-0.03 J) - Fig. 1d, e; Fig. 2 c,d,e; Fig. 3, partial to the full erasure of deep scratches, and reduction in the surface roughness to Ra=2.5-3 μm was obtained after the LESD process. However, the lower pulse energy (E <0.02 J) (Table 3, Fig. 3) is not always sufficient for the electrode melt to fill the unevenness, pores and cavities of the initial surface and the deepest traces of pre-treatment cannot be completely deleted.

At the higher impulse energy - Tables 4 and 5 and Figs.1b,c; Fig. 2b; Fig. 3, the traces of DLMS are erased almost completely, but the roughness of the coatings shows a tendency to increase – Table 4, 5 and Fig. 3 and the parameter Ra accepts values up to 4.5 -5 μm. In LESD with AlSi electrodes, the initial roughness of DLMS surfaces of both titanium and martensitic steel in regimes with pulse energy up to 0.02-0.03 J can be reduced up to 3 times, and in LESD with NWW electrodes - up to two times.

A comparison of the coatings from the used NWW electrodes with different ratios between the components shows close values of the roughness parameters. At E=0.02-0.03 J, the lowest values of the

roughness parameters have the coatings from the NWW15T20 electrode, but the differences in the roughness of the coatings from the "NWW" electrodes are negligibly small.

In Fig. 4 gives pictures of cross- section of the coatings from the NWW electrodes applied with 3 passes at pulse energy 0.04 J (mode 3-Table 2) on 1.2709 steel and on Ti6Al4V. It can be seen that a dense layer deeply filled the pores left after the DMLS treatment.



a) LESD on 1.2709 steel (δ≈28 µm) b) LESD on Ti6Al4V alloy (δ≈23 µm)

Fig. 4. Cross- section microphotographs of microstructure of coatings from NWW10T10B10 electrodes

The micro-hardness (HV) of the coatings is up to 2-4 times higher than that of the non-coated substrates and it exceeds in value the respective initial hardness of the aluminum electrodes. One can notice also a tendency of increasing the micro-hardness upon increasing the energy of the impulses (Table 4 and 5), with the measured average microhardness of coatings on 1.2709 steel being higher than that of titanium alloys.

3.2. Phase composition of coatings

The main phases in the compositions of the "NWW" coatings on TiGR2 are Ti, TiN, WC1-x, TiB_2, $TiC_{0.7}N_{0.3}$, WB, Cr_2B_3, TiC1-x, NiB, NiTi, $Cr_{0.2}Ti_{0.3}$. There are also registered small quantities (traces) of newly formed wear-resistant compounds and intermetals such as: TiB, B_4C, AlN, Si_3N_4,Ti(C,N), CoB, Ni_3Ti, CrNiW, Ti_3Ni, and Ti_2O. It is found that under the action of the spark plasma discharges, the components of the electrode material are decomposed partially, forming many new compounds. The palette of nitrides, carbides and carbonitrides, in relatively a little amount shows that in the process of LESD titanium reacts with nitrogen from the air and carbon from the electrode material forming of new wear resistance carbides and nitrides. XRD models of coatings applied with different impulse energies differ mainly in the intensity and width of the characteristic peaks of iron and intermetallic phases.

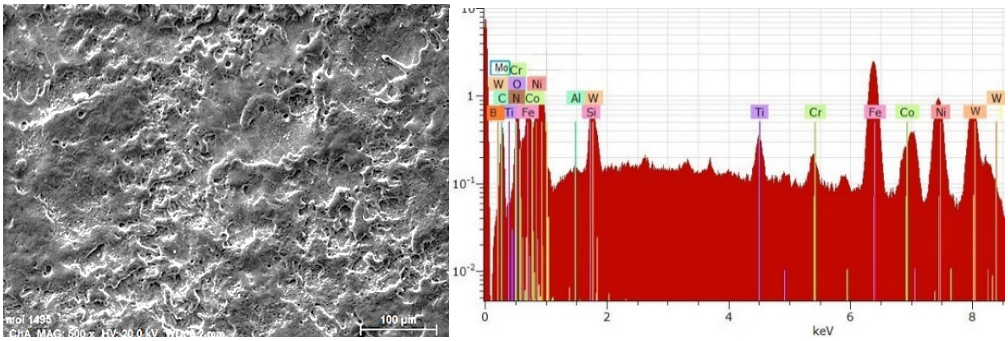
The registered broadening of the diffraction peaks of Al and Ti reflects the formation of both solid solutions and new compounds in the resulting anode-cathode molten mixture, as well as a reduction in the size of the structure, reaching an amorphous phase. Since there are also peaks in the wider-angle zones that give an indication of the presence of crystallites, it can be concluded that the coatings have a crystalline-amorphous structure. The degree of amorphousness is close than that of AlSi coatings, and increases with increasing pulse energy. The main phases in the compositions of the AlSi coatings are: α-Ti, Al, Al_3Ti, Ti_5Si_3, $AlSi_3Ti_2$, $TiN_{0.26}$. In small quantities are registered Al_2O_3 TiC1-x, TiCxNy, TiO_2, TiO. The resulting Al-based amorphous metal alloys are also favorable for the mechanical properties and wear resistance of the coatings.

Similar results were obtained at LESD on 1.2709 DMLS steels, but at LESD with "NWW" type electrodes, the amount of titanium carbides, borides and carbonitrides was higer than that of coatings on TiGR2 substrates. The main registered phases in the composition of the NWW coatings are: martensite-α-Fe, austenite -γ-Fe, Cr-Ni-Fe-C, WC_{1-x}, Cr_7C_3, WB_2, WB, TiB_2, $TiCo_3$, traces of W_2C, Fe_2B, CoB, $FeNi_3$, CrNiW, CrFe, Cr_3B_4 ,B_4C are also registered. The characteristic diffraction peaks of the α-Fe, and γ-Fe are present for all coated samples. They are broadened and displaced, which indicates the

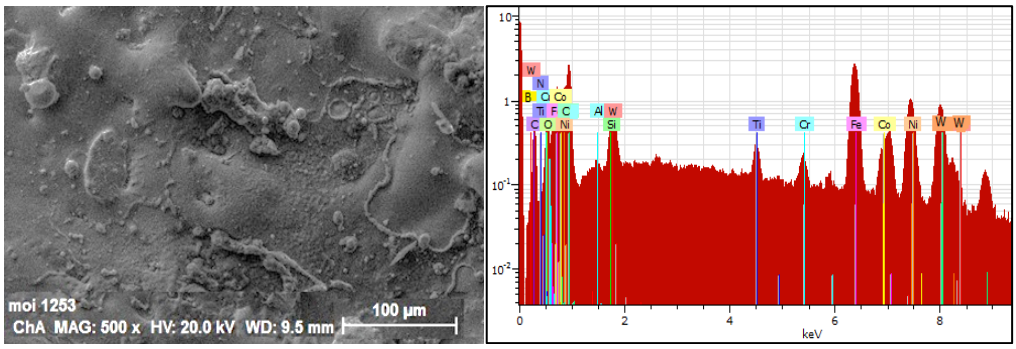
presence of superdispersed to an amorphous structure, solid solutions, crystal defects, and internal stresses (Penyashki, Kostadinov et al.2020).

The main registered phases in the composition of the AlSi coatings on 1.2709 steel are: (Fe, Ni), AlFe, FeSi, Al_5Fe_2, $Al_{3.2}Fe$, $AlFe_{0.23}Ni_{0.77}$, $Fe_{0.7}Ni_{0.3}$, AlO, Al_2O_3, FeNi**.** AlCo, $Fe_{0.9}Si_{0.05}$, $FeNi_3$, $NiAl_3$, AlNi, $Al_{0.9}Ni_{1.1}$, $AlFe_{0.23}Ni_{0.77}$, $Al_{2.67}O_4$, AlO are found in small quantities, also and traces of AlN, Si_3N_4. The presence of Al_2O_3, as well as traces of AlN and SiN, indicate that aluminum have reacted with oxygen and nitrogen in the air to form wear-resistant compounds. The average crystal size, calculated by Scherer's formula, varies from 15 to 90 nm for the different phases, which shows that the new phases obtained in the electrospark coatings have a nanocrystalline structure.

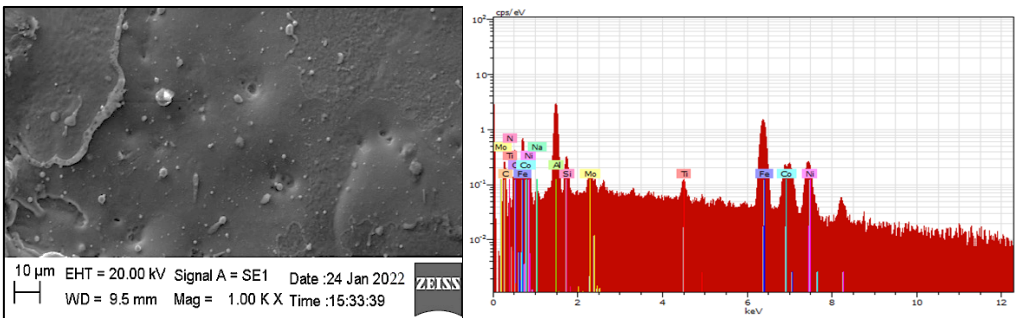
From the X-ray data on the coatings applied with the new multicomponent electrodes, it is found that the phase composition of 1.2709 steel is enriched with more carbides and borides than in LESD with AlSi electrodes and approaches that of high-speed steels, which suggests a significant improvement in the operational properties of layered surfaces.



a) SEM micrograph and EDX spectrum of coated T-GR2 DMLS substrate with NWW15T20B10 electrode



b) SEM micrograph and EDX spectrum of coated 1.2709 DMLS steel with NWW15T20B10



c) EDX spectrum of coated 1.2709 DMLS steel with AlSi electrode

Fig. 5. SEM micrographs and EDX spectrum of coatings from NWW15T20B10 electrode on Ti6Al4V alloys (a) and 1.2709 steel (b), and coated with AlSi electrode 1.2709 steel (c) at E=0.03 J

The presence of the constituent elements of the registered phases is confirmed by the energy dispersion analysis of the coatings (Fig. 5) where the peaks of the elements are clearly visible. SEM observations of the coatings on 1.2709 steel show that the presence of iron in the coating indicates melting of the base. Judging by the distribution of iron and titanium, it can be assumed that titanium mainly forms round carbides and borides. Based on the obtained data, it can be concluded that Ni, Co, Cr, and other elements that do not participate in the formation of carbides and borides form a solid solution with iron. The formation of a metal matrix in the form of a solid solution is confirmed by the distribution of Ni, Cr, Co and Fe. The microhardness of the NWW electrode coatings on Ti-GR2 is 8.5-14 GPa. However, there are individual measured values up to 17.5 GPa. The highest microhardness has the coatings obtained in LESD with the electrodes containing higher amounts of TiB_2 and WC.

The new phases formed in the process of spark-plasma discharges presuppose stronger bonding with the substrate, higher microhardness, and correspondingly higher wear resistance.

As the pulse energy increases, the degree of dispersion and the amount of newly obtained intermetallic phases increase. By appropriate selection of the pulse energy and the pulse parameters, it becomes possible to achieve a purposeful synthesis of certain phases. Therefore, the use of abouve electrodes provide improved properties of the surface layer, due to the fine-grained structure, the new compounds and amorphous phases in the composition of the coatings.

3.3. Wear Resistance of coatings

Fig. 6 shows the mass wear of the coatings of the studied electrodes as a function of the friction path.

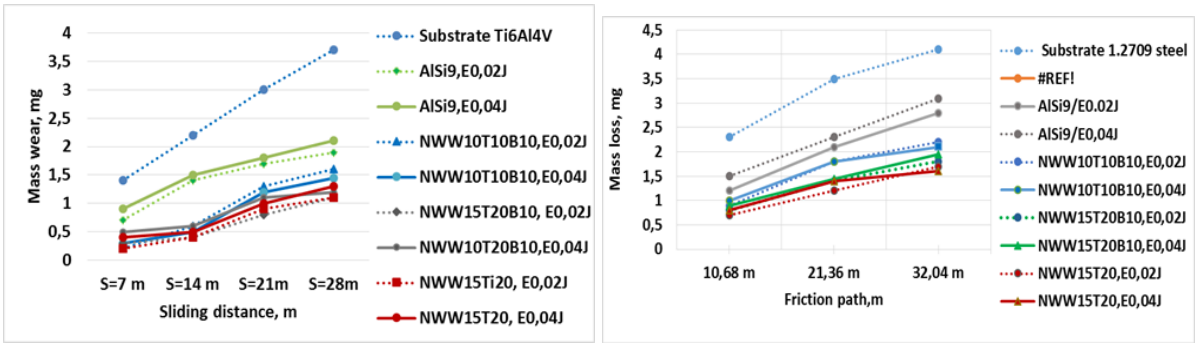


Fig. 6. Wear of ESD coatings on Ti-GR2, (P=5 N) and 1.2709 DMLS steel (P=10 N).

From the obtained results, it is visible that the mass wear of the coated samples of titanium alloy is 2-4 times lower than that of the uncoated ones. The wear of the coated steel specimens is similar. The changes of the wear rate, the wear intensity, and the wear resistance of the coatings are similar.

Amorphous-micro-nanocrystalline composite coatings from NWW15T20B10 electrodes showed the lowest wear- up to 4 times lower than that of the uncoated samples, followed by the coatings from NWW15T20 electrodes, apparently due to the higher amount of WC and TiB_2 in their composition. The ultra-hard B_4C in the composition of the NWW electrodes has a dual role. The particles transferred to the initial state firmly stuck in the metal matrix of the coating increase its resistance to wear. On the other hand, the partial dissociation of B_4C in the transfer process serves as a donor of B and C and helps the formation of new borides and carbides such as WB, Cr_3B_4, CrNiW, Fe_2B CoB, which further contribute to the increase in wear resistance of the coating.

The mass wear of coatings from AlSi electrodes is up to 2-2.5 times lower than that of the uncoated samples. In that, the differences in the wear of the layers obtained at the two values of the pulse energy are small.

As can be seen, (Fig. 6), the time to reach the mass wear of 2 mg of the coated samples with NWW15T20B10 electrodes at energy 0.02 J is about 2 times longer than that of the layered with AlSi

electrodes and to 4 times longer than that of the uncoated ones. However, the differences in the wear of the samples coated with the used different NWW electrodes are relatively small. Furthermore, in this case the classic surface microgeometric indicators (Ra, Rz, Rt, Rq) do not reflect the actual situation of the frictional contact. The coatings from NWW15T20 and NWW15T20B10 electrodes have higher Ra, Rz, Rt values than those of AlSi coatings, but their wear resistance is also higher.

The obtained results testify to the suitability of the investigated electrode materials for creating quality LESD coatings on DMLS surfaces both in terms of their parameters – thickness, topography, mechanical properties and and their wear resistance. The analysis of the results leads to the conclusion that through the new electrodes and coatings, prerequisites and possibilities have been created for the purposeful formation of predetermined properties of the surface of the friction contact. The coatings obtained with the NWW electrodes make it possible not to use complex and expensive methods to remove the defects and deficiencies of the DMLS surface, but to carry out the treatment by LESD in such a way as to guarantee both the removal of the surface defects and the required resistance of wear.

4. CONCLUSIONS

1. At LESD with NWW and AlSi electrodes on Ti and 1.2709 3D printed steels, amorphous-crystalline coatings are obtained with a controlled thickness of up to 25 μm, with more than twice lower roughness and up to 3-4 times higher hardness and wear resistance than those of the original 3D surfaces.

2. The used electrodes and values of the LESD process parameters show the possibility of achieving the best quality of the treated surfaces and the highest microhardness and wear resistance.

3. The use of AlSi electrodes results in lower surface roughness and more complete removal of initial surface defects after 3D printing, while with NWW electrodes the surface is more uneven, but the hardness and wear resistance are higher than those of AlSi electrodes.

4. With both types of electrodes, the presence of amorphous and nano-sized structures and the synthesis of new phases were registered in the composition of the coatings, which suggest better adhesion with the base and wear resistance. When using NWW electrodes, due to their multi-component nature, the amount of newly formed intermetallic, carbide, boride and nitride phases is significantly higher.

5. The titanium and steel 3D surfaces with coatings of NWW15T20B10 and NWW15T20, which have an increased content of WC and TiB_2, show the highest microhardness and wear resistance, and the highest thickness show the coatings of NWW10T10B10.

ACKNOWLEDGMENTS

The present work is based on researches that are funded from the Bulgarian National Science Fund of the Ministry of Education and Science under the bilateral project Bulgaria- Russia “Improving the Quality of Surfaces Obtained by Additive Technologies by Reactive Electro-spark Processing” and the project “Technological Features and Regularities of Creation of New High Wear Resistant Composite Coatings on Titanium Alloys by Electrical Spark Deposition Process”.

REFERENCES

1. Aloshin, NP, Murashov, VV, Yevgenov, AG, Grigor'yev, MV, Shchipakov, NA, Vasilenko, SA & Krasnov, IS 2016, „Classification of defects in metallic materials, synthesized by the method of selective laser melting, and the possibility of other methods for their detection“, *Defektoskopiya*, № 1, pp. 48-55,(in Russ.).
2. Bogers, M, Hadar, R, & Bilberg, A 2016, “Additive manufacturing for consumer-centric business models: implications for supply chains in consumer goods manufacturing”, *Technological Forecasting and Social Changes*, Elsevier, vol. 102(C), pp. 225-239.

3. Laplume, A, Petersen, B & Pearce, J 2016, "Global value chains from a 3D printing perspective", *Journal of International Business Studies*, Vol. 47, no. 5, pp. 595-609.
4. Freedman, Dh 2013, „Layer by Layer", *Technology Review: Academic Search Premier*, vol.115 (1), pp. 50-53.
5. Monkova, K, Zetkova, I, Kučerová, L, Zetek, M, Monka, & Daňa, M 2019, "Study of 3D printing direction and effects of heat treatment on mechanical properties of MS1 maraging steel", *Archive of Applied Mechanics*, vol. 89, no 5, pp. 791-804.
6. Zaytsev, V & Polupan, A 2020, "Selections parameters of selective laser melting for metal powders", *Open Information and Computer Integrated Technologies, Open Journal Systems* (OJS), no. 89, pp. 48-58.,
7. Shipley, H, McDonnell, D, Culleton, M, Lupoi, R,O'Donnell, G & Trimble, D 2018, "Optimisation of process parameters to address fundamental challenges during selective laser melting of Ti-6Al-4V", A review. *International Journal of Machine Tools and Manufacture,* 128. 10.1016/j.ijmachtools.2018.01.003.
8. Sufiyarov, VSh, Borisov, EV, Polozov, A & Masailo, DV 2018, „Control of Structure Formation in Selective Laser Melting Process", *J Tsvetnye Metally*, no. 7, pp. 68-74 (in Russ.).
9. Yasa, E. & Kruth, J 2011, "Application of Laser Re-melting on Selective Laser Melting Parts", *Adv. Prod. Eng. Manag*. Q. vol 6, no. 4, pp 259–270.
10. Ramos-Grez, JA, & Bourell, DL 2004, "Reducing Surface Roughness of Metallic Free Form Fabricated Parts Using Non-tactile Finishing Methods", *Int J of Materials and Product Technology*, vol.21, pp. 297-316.
11. Tsvetkova, EV, Bazaleeva, KO, Chekin, IS, Klimova-Korsmik, OG, & Zhidkov, AS 2020, "Nitriding of steels of various structural classes manufactured by laser additive technologies", Izvestiya. *Ferrous Metallurgy*, vol. 63, no.1, 63-70. (In Russ.) https://doi.org/10.17073/0368-0797-2020-1-63-70].
12. Grabarczyk, J, Batory, D, Kaczorowski, W, Pązik, B, Januszewicz, B, Burnat, B, Czerniak-Reczulska, M, Makówka, M. & Niedzielski, P 2020, "Comparison of Different Thermo-Chemical Treatments Methods of Ti-6Al-4V Alloy in Terms of Tribological and Corrosion Properties", *Materials*, vol. 13, no. 22, p. 5192.
13. Penyashki, T, Kostadinov, G, Kandeva, M, & Radev, D 2020, "*Electro spark and gas flame layering opportunities and application*", Roll Company Publishing House, Sofia, 190 p. (in bulgerian).
14. Penyashki, T & Kostadinov, G 2013, Enhancing durability and resources agricultural machinery using electrospark hardening, *Agricultural Engineering* (Bulgaria), pp. 48-55.
15. Mukanov, SK., Kudryashov, AE & Petrzhik, MI 2021, "Surface Modification of Titanium VT6 Alloy Obtained by Additive Technologies Using Reactive Electrospark Treatment", *Physics and Chemistry of Material Processing*, no. 3, pp. 30-39.
16. Kostadinov, G, Penyashki, T, Kamburov, V, Kandeva, M, Mikhail IP & Kudryashov, AE 2021, "Possibilities for improving the surface quality of structural steels, invar and titanium alloys through reactive electrospark treatment with electrodes of an aluminum-silicon alloys", *Materials, Methods & Technologies*, vol. 15, pp. 105-122.
17. Penyashki, T, Kostadinov, G, Kalitchin, Zh., & Kandeva, M 2022, "Ecological aspects of electrospark deposition technologies for improvement of the metal surfaces quality prepared by 3D printing. Part I, Topography and microhardness of the coatings", *Journal of Environmental Protection and Ecology*, vol. 23, no. 3, pp. 1039–1048.
18. Antonov, B, Panayotov, St, & Lyutakov, O 1980, "*Apparatus for the spark deposition of metals*", US Patent 4226697.

19. Penyashki, T, Radev, D, Kandeva, M & Kostadinov, G 2020, "Structural and tribological properties of wear resistant coatings obtained by electrospark deposition", *IOP Conference Series Materials Science and Engineering* 724:012015, DOI: 10.1088/1757-899X/724/1/012015.

20. Penyashki, T, Radev D, Kandeva, M & Kostadinov, G 2019, "Structural and Tribological Properties of Multicomponent Coatings on 45 and 210Cr12 Steels Obtained by Electrospark Deposition with WC-B4C-TiB2-Ni-Cr-Co-B-Si Electrodes", *Surface Engineering and Applied Electrochemistry,* vol. 55, no. 6, pp. 638-650, DOI: 10.3103/S1068375519060097.

21. Kamburov, V, Valkanov S, Mateev, V, Marinova, I, Dimitrova, R, Nikolo,v A, Penyashki, T, Kostadinov, G & Kandeva, M 2021, "Microstructural Analysis and Electroresistance Investigation of Hardalloyed Electrospark-Deposited Coatings on TiAl6V4 Alloy", *12th National Conference with International Participation (ELECTRONICA)*, 1-6, https://ieeexplore.ieee.org/abstract/document/9513676,

22. Milligan, J, Heard, DW, & Brochu, M 2010, "Formation of nanostructured weldments in the Al-Si system using electrospark welding", *Applied surface science*, vol. 256. no. 12. pp. 4009–4016.

23. Cadney, S, Goodall, G, Kim, G, Moran, A & Brochu, M 2009, "The transformation of an a Al-based crystalline electrode material to an amorphous deposit via the electrospark welding process", *Journal of alloys and compounds,* vol. 476. no. 1-2. pp. 147—151.